Advanced Ceramics Progress: Vol. ?, No. ?, (Season 202?) ??-??

Materials and Energy Research Center
MERC

Contents lists available at ACERP

Advanced Ceramics Progress

Journal Homepage: www.acerp.ir

Original Research Article

Investigation on the band gap of centered square phononic crystals

Bentolhoda Amanat [a, *], Mohammad Reza Kazerani Vahdani [b]

[a] *Assistant Professor, Department of Physics, Payame Noor University, Tehran, Iran*
[b] *Associate Professor, Faculty of Naval Aviation, Malek Ashtar University of Technology, Iran*

* Corresponding Author Email: amanat@pnu.ac.ir (B. Amanat)

URL: http://www.acerp.ir/article_90833.html

ARTICLE INFO

Article History:

Received ? Month 202?
Received in revised form ? Month 202?
Accepted ? Month 202?

Keywords:

phononic crystal
band gap
piezocomposite
filling fraction

ABSTRACT

The periodic structure of 1-3 piezocomposite phononic crystal minimize the influence of coupling of the parasitic modes on the deliberately excited plane modes and prevent the propagation of unwanted Lamb waves. In this article, the band structures of centered square phononic crystals of PZT-5H rods in polyethylene terephthalate matrix have been studied using the numerical method of finite elements. In particular the phoninic band gaps of the system have been investigated as functions of the volume of the PZT element at the center of the unit cell of the considered crystal, under the condition of constant filling fraction of PZT rods. The results indicate that the band structure of the system contain three gap whose width vary by the volume. These gaps have extended in the (normalized) frequency range 1100 m/s to 2530 m/s Particularly it is shown that when the all PZT rods of the system are of the same size, the maximum achievable band gap of the system attains.

https://doi.org/10.30501/acp.2018.90833

1. INTRODUCTION

Today, piezocomposite materials are used in many engineering applications and smart structures. The idea of piezocomposite materials was presented in 1978 by Newnham et al. which has received much attention and achieved significant achievement [1]. In piezocomposite structure, a piezoelectric material with high piezoelectric properties such as PZT and PMN-PT generally acts as active phase and a polymer material such as epoxy resin, polyethylene, etc. acts as an inactive phase [2] [3]. Using the connection concept proposed by Newnham, these materials are classified into 10 types of piezocomposites [4]. One of the most famous and widely used of these materials is 1-3 piezocomposite.

Superior properties of piezocomposites such as low acoustic impedances, (from 5 MRayl to 27 MRayl), high coupling coefficients (usually 0.61 to 0.75), high bandwidth and lower Qm have made these materials widely used in high frequency ultrasound transducers, medical imaging and sonar systems [5] [6]. Periodic structure of piezocomposites causes the formation of certain stop bands or band gaps in the frequency spectrum of these structures. The existence of these band gaps has caused the propagation of elastic waves in heterogeneous media to attract the attention of many scientists in the past years [7]. In fact, the large band gaps in piezocomposites are suitable for many applications, such as elastic and acoustic filters, transducer structres, control of noise, and vibration shields [8]. For instance,

Please cite this article as: Lastname1, F1., Lastname2, F2., Lastname3, F3., "Title must be Times New Roman, 14, Bold, Justify", ***Advanced Ceramics Progress***, Vol. ?, No. ?, (202?), ??-??. https://doi.org/10.30501/acp.2018.90833

by setting the frequency of the thickness mode of piezocomposites in band gaps, it is possible to minimize the coupling with parasitic modes such as lateral modes and prevent the propagation of Lamb waves. Therefore, considerable research has been devoted to increasing the band gap widths [9] [10] which strongly depends on the physical properties, size and shape of constituent phases [11].

Hou et al. [12] investigated the elastic band gap structure of a two-dimensional acoustic crystal containing piezoelectric materials and analyzed the piezoelectric effects on the band gaps. Qian et al. [13] studied the dispersion relations of horizontal shear wave propagation in a periodic layered piezoelectric structure for cases of wave propagation in normal and tangential directions to the interface. Silva et al [14] investigated the maximization of absolute elastic wave gap width in designed piezocomposite materials using topology optimization. Zheng Hua et al. [15] compared the band gaps in two-dimensional piezocomposite with 1-3 connection family of piezoceramic rods with circular and square cross-sections. Sigmund [9] [16] applied the method of topology optimization to design periodic materials and structures with acoustic band gaps to minimize the structural response along the boundaries or maximize the response at certain boundary points. Halkjer et al. [17] maximized the acoustic band gap for infinite periodic beam structures modeled by Timoshenko beam theory, for alternating, thick and medium thickness plates and for finite thick plates. Jensen et al [18] maximized the bandgap size for shear waves in the Mindlein plane. Evgrafov et al. [19] applied topology optimization to the design of 2D and 3D phononic (elastic) materials, focusing on surface wave filters and waveguides. Other issues related to the propagation of sound waves in two-dimensional and three-dimensional piezoelectric periodic structures have been mentioned in various researches [20] [21] [22] [23].

Most of the researches that preformed in the past, were mainly based on three main axes. First, changing the piezoceramic filling fraction, which causes changes in piezocomposite parameters such as coupling coefficient, characteristic impedance, effective density, and longitudinal velocity. Second, the change in the geometric shape of piezoceramics and the use of different geometric shapes, the problem of this method is that you cannot have a good control over the adjustment of these band gaps. Third, the change in the ingredients of the piezocomposite, which, like the second case, causes a sudden change in the band gap parameters, and it is not possible to have good control over the adjustment of the band gaps.

In this research, we suggest a 1-3 piezocomposite of centered cubic crystal structure and investigate the effect of volume fraction of different phases of piezoelectric rods on the band gaps at constant ceramic filling fraction. In this analysis, Bloch-Flocke theory [24] and finite element analysis were used to investigate the dynamic behavior of two-dimensional piezocomposite unit cells for calculation of the band gap. In this research, we have presented a structure that can be used to control the width of band gaps without changing the filling fraction and only by changing the ηs. It is shown that in the case of η=50%, we can reach the maximum gap bandwidth.

2. Problem explanation and finite element modeling

The system considered in this study is a 1-3 piezocomposite structure composed of a square lattice of lattice constant a and a unit cell containing a couple of rods of PZT-5H with circular cross-section and different radii, represented by white and gray color in Figure 1. The PZT rods are considered to embed in a polymer matrix of polyethylene terephthalate.

Due to the periodicity of the considered crystal and its infinite size along x and y axis, the mechanical displacements u_i and electric potential φ obey the Bloch relation (Equation (1-2)) [15]:

$$u_i(x+ma_1,y+pa_2) = u_i(x,y,z)\exp(-jk_xma_1)\exp(-jk_ypa_2) \quad (1)$$

$$\varphi(x+ma_1,y+pa_2) = \varphi(x,y,z)\exp(-jk_xma_1)\exp(-jk_ypa_2) \quad (2)$$

where the components of the Bloch wave vectors in the x and y directions are shown by kx and ky, respectively and m and p are integer.

The above mentioned periodical boundary conditions make it possible to limit the calculations just to a single unit cell. The square unit cell of the system is considered as depicted in Figure 1-b. The cell contains two different rode one represented by four quarter circles of radius R_A at the corners and a full circle of radius R_B in the center which hereafter are called rod A and rod B respectively. The polarization axis of the piezoelectric rods is considered perpendicular to the plane of the unit cell.

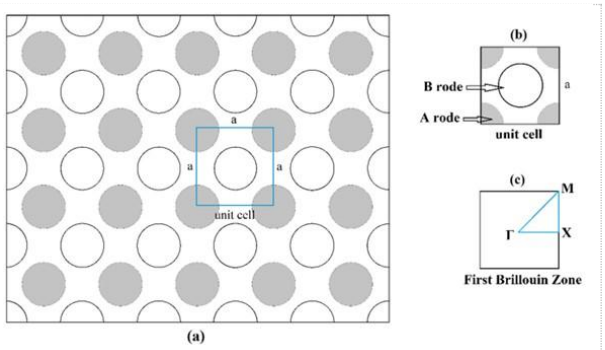

Figure 1. According to the schematic, (a) the proposed 1-3 piezocomposite network model, (b) the unite cell of the network, (c) show the first Brillouin zone. Gray circles are rode A and white circles are rode B. we change the size of the

gray circles and the white circles in such a way that the filling fraction of the piezocomposite remains constant.

For the above considered piezocomposite, the filling fraction of the piezoceramics phase, which defined as the ratio of the volume of the piezocomposite rods in the unit cell to the total volume of the unit cell, is equal to Equation(3).

$$(\pi(R_A^2 + R_B^2)/a^2) \quad (3)$$

In addition, we define here the volume fraction of the rod B as the ratio of the volume of rod B to the summation of the volume of the rods A and B in a unit cell and represent it by η (Equation(4)) . Based on the radius of the rods one has

$$\eta = \frac{R_B^2}{R_A^2 + R_B^2} \quad (4)$$

The aim of this paper is to investigate the band structures of the above mentioned phononic crystal as a function of η in order to find the optimum value of η for which the band gap attains their maximum. To this end and for the sake of simplicity, the filling fraction is considered constant equal to 50% everywhere in this research. In the other word as the R_b increases by increasing η , R_a must be decreases in such a way that the filling fraction remains constant.

Due to the complex topology of this structure, a numerical method, such as the Finite Element Method (FEM), is necessary for analyzing the vibrational properties of the structure. The finite element numerical method has been well developed for linear piezoelectric materials and have been widely used in analyzing piezocomposites. Thus, in this study the FEM would be used in studying band structures of the considered composite. To this end the unit cell is divided into a mesh of triangular elements connected by nodes as represented schematically in Figure 2.

In the absent of external forces and by considering monochromatic time dependent exp(jωt) the general piezoelectric problem is written as Equation (5) [14].

$$\begin{bmatrix} K_{uu} - \omega^2 M_{uu} & K_{\varphi u} \\ K_{\varphi u} & K_{uu} \end{bmatrix} \begin{pmatrix} u \\ \varphi \end{pmatrix} = \begin{pmatrix} 0 \\ 0 \end{pmatrix} \quad (5)$$

where K_{uu} and M_{uu} are the stiffness and mass matrixes of the fully elastic part of the problem, respectively. $K_{\varphi\varphi}$ represents the pure dielectric part and $K_{u\varphi}$ is the piezoelectric coupling matrix. As mentioned, the translational symmetry of the lattice allow to reduce the problem the first Brillouin zone, Figure 1 (b). To obtain the dispersion diagrams, the wave vector varies inside the first Brillouin zone for a given propagation direction which as usual can be reduced using the symmetry properties of the system to the first irreducible Brillouin zone. For a square lattice of constant a, the first Brillouin zone is defined by $-\pi/a<kx<\pi/a$ and $-\pi/a<ky<\pi/a$ and the band structures are calculated along the M-Γ-X-M path (see Figure 1(c)). To confirm the accuracy of the results the mesh sizes have been refined repeatedly until the angular frequency convergence has been obtained.

TABLE 1. Characteristics of the materials used in the calculations [25] [15]

		PZT-5H		polyethylene terephthalate
Elastic constants ($10^9 Nm^{-2}$)	C_{11}	121	Young's modulus	7×10^9
	C_{33}	117		
	C_{44}	23		
	C_{13}	84.1		
	C_{12}	79.5		
Piezoelectric constants (Cm^{-2})	e_{15}	17	Poisson's ratio	0.44
	e_{31}	-6.5		
	e_{33}	23.3		
Dielectric constants (10^{-10} F m^{-1})	ε_{13}	150	Mass Density (kg/ m^{-3})	1430
	ε_{33}	130		
Mass Density (kg/ m^{-3})	ρ	4500		

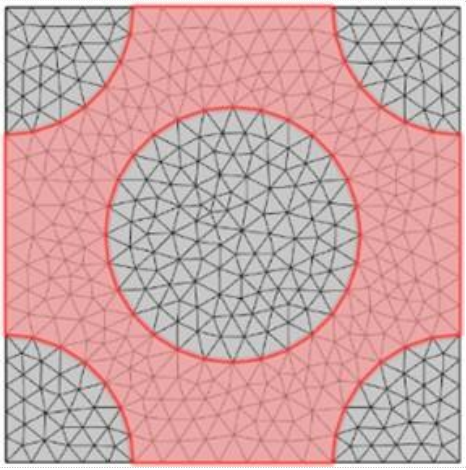

Figure 2. A view of a meshed unit cell.

2. Numerical simulation and discussion

In this section, the results of the variation of the volume fraction η on the band structure of the piezoelectric phononic crystal, introduced in the last sections, are presented and discussed. By considering the total filling fraction of the PZT-5H rods as constant equal to 50%, and altering the η from 0 to 50% the band structures are obtained by calculating the lowest 20 bands of the system utilizing the finite element analysis. The material parameters used in the calculations are tabulated in Tables 1. The results are as follow. It should be noted that since the rods in a unit cell are consist of a same type of piezoceramic material, i.e. PZT-5H, it is expected that band structure for η values greater than 50% would be similar to their counterparts of η<50%. In the other word, for example the band structure of η=70% match that of η=30% because the only difference between the unit cell in this case is that the volume of rods A and rods B are replaced. The bands are calculated along the path M-Γ-X-M about the irreducible Brillouin zone of the square lattice and plotted in term of the product of frequency and lattice constant f × a versus the wave vector K along the first irreducible Brillouin zone, see Figure 1-c. It is inferred that the existing band gaps extend across the Brillouin zone as stated by Vasseur et al. [24].

Figure 3 illustrate the band structures of the considered 1-3 piezocomposite in the limiting case η=0, which is corresponding to a simple square lattice. As can be seen in Figure 3, there exist just one complete band gap between third and fourth band. The gap extended in the frequency range 1100<f.a<1500 with relative bandwidth 31%.

By increasing from zero the volume of rod B starts to grow from zero which in addition with the constant filling fraction 50% causes the volume of rod A to decrease.

In Figure 4 (a) the band structure for η=5% have been represented. It is shown in this case that the magnitude of band gap between third and fourth bands decrease to 209m/s. This band starts from 1105 m/s to 1314 m/s with relative bandwidth 17%. Although this gap is squeezed by increasing η from zero, another band gap starts to appear between tenth and eleventh bands. This gap lies in the frequency range 2296 m/s to 2527 m/s with relative band gap 9.8%. The presence of the later gap could be attribute to the emergence of rods B in the middle of the unit cell instead of decrease in the volumes of rod A. To check this, we evaluate the band structures for very small values of η, not shown here, and observe that the later gap starts to grow immediately as η increases from zero. Since for these small values of η the volume of rod A does not change considerably, it is reasonable to attribute this band gap to the new scattering center produced in each unit cell. (The number in the right of each Figure is the bandwidth of band gap)

By increasing η to 10% a third gap start to emerge as presented in Figure 4 (b). As indicated in this figure this gap lies between 6th and 7th bands with lower edge 1737m/s and relative bandwidth 0.4%. Although in this case the lower limit of first band gap remains unchanged with respect to =5% case, its band width decreases to 95m/s as a result of descending the 4th band. Contrarily the second band gap now grow to 262m/s with relative bandwidth 10.9% due to descending 10th band and rising 11th band.

By further increase of η to 20%, the first band gap is closed completely as a consequence of the downward movement of the fourth (in addition with the fifth and sixth) bands although the first, second and third bands remains almost unchanged. As presented in Figure 4c, here the bandwidth of 2nd band gap shrinks symmetrically to 131 m/s so that its lower edge increases to 2362 m/s. On the other hand, although both the maximum of 6th band (1597m/s) and the minimum of 7th band (1791m/s) have been decreased, the width of third band width increases to 194m/s.

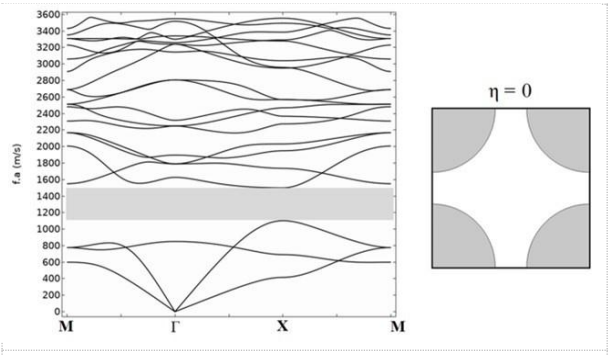

Figure 3. Dispersion diagram and elastic band structure for XY vibration modes in a typical 1-3 piezocomposite in 50% piezoceramic filling fraction, which does not have rode A circles (η=0)..

TABLE 2. Specifications of materials used and different values of η

Figure	η	Polymer material	piezoceramic material	Piezoceramic filing fraction
3	0	polyethylene terephthalate (PET)	PZT-5H	50
2-(a)	5			
2-(b)	10			
2-(c)	20			
2-(d)	30			
2-(e)	40			
2-(f)	50			

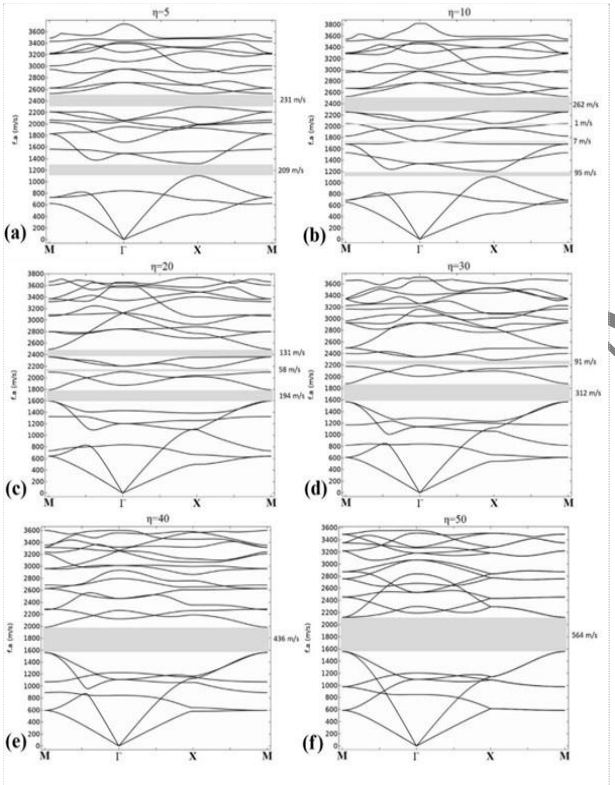

Figure 4. Dispersion diagram and elastic band structure for XY vibration modes in a typical 1-3 piezocomposite in 50% piezoceramic filling fraction.

The width of the third band gap grows continuously as η increases to 50% that reaches its maximum, see Figures. 4-b, c, d, e, f. At η=50% the third gap extended in the frequency range 2122<f.a<1558 with band width equal 564m/s and relative bandwidth 31%. This can be easily found that since the 5th and 6th bands remain almost unchanged, the widening of this gap occurs as a direct result of the shift of 7th band to the higher frequencies. In addition, there exist a narrower band gap just above 7th band from η=10% to η=40%, Figure 4-b, c, d, which is faded as η increases to 40%. The maximum relative bandwidth of this gap is 4.3% whose minimum at 2234m/s occurs at M point of Brillouin zone for η=35% (show in Figure 6). An interesting feature of the case η=50% is the dual degeneracy of each band in the X-M range. In the other word the six bands which exist in the ranges M-Γ and Γ-X converge so that just three band are observed in X-M range. This happens due to the fact that, for η=50% the centered square lattice under consideration transforms into a simple square lattice of lattice constant $a/\sqrt{2}$ whose axis rotates $\pi/4$ with respect to the axis of the centered square lattice considered so far. The Brillouin zone of this lattice is depicted in Figure 5 along with that of the original centered square. The calculation of band structure for the simple square lattice mentioned above along with the (unconventional) directions of Figure 5 shows complete match with the case η=50%.

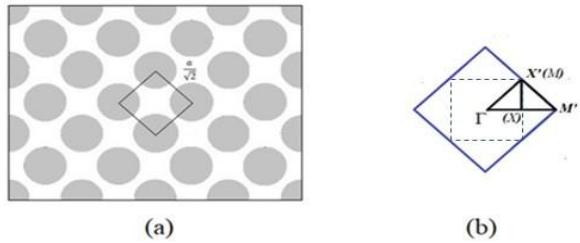

Figure 5. According to the schematic, (a) the unit cell of simple square lattice associated with = 50% (solid line), (b) The B.Z. corresponding to the simple square in addition with the B.Z. of a centered square lattice constant a of fig.1 (The dotted lines show the Brillouin zone in Figure 1.)

TABLE 2. Specifications of each band gap for different η

	1st Band gap			2nd Band gap			3rd Band gap		
η	Band end (m/s)	Band start (m/s)	Bandwidth (m/s)	Band end (m/s)	Band start (m/s)	Bandwidth (m/s)	Band end (m/s)	Band start (m/s)	Bandwidth (GHz)
0	1500	1100	400						
5	1314	1105	209	2527	2296	231			
10	1202	1107	95	2530	2268	262	1744	1737	7
15	1138	1110	28	2518	2306	212	1772	1665	107
20				2493	2362	131	1791	1597	194
25				2457	2424	33	1829	1580	249
30							1881	1569	312
35							1931	1564	367
40							1984	1548	436
45							2052	1559	493
50							2122	1558	564

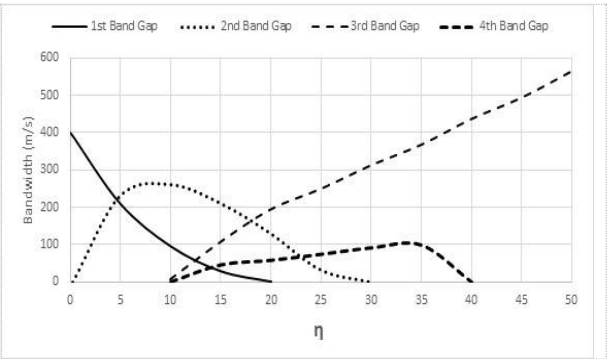

Figure 6. The width of the first five bands in terms of different values of η at the filling fraction F=50%

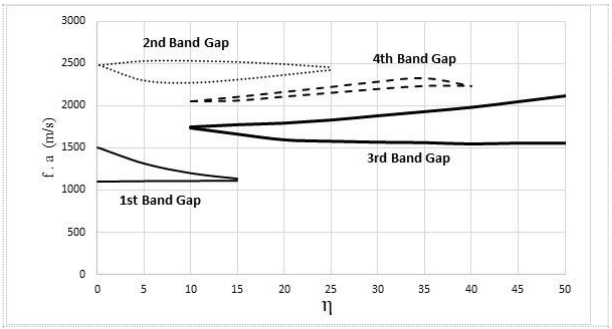

Figure 7. The open points, close points and width of the band gaps at the filling fraction F=50% versus η

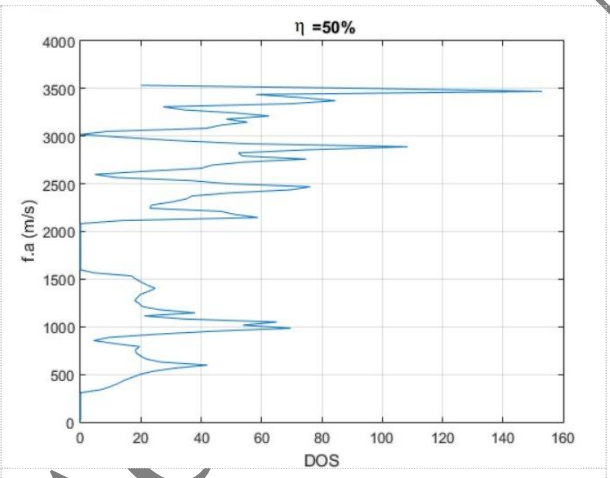

Figure 8. The density of states at the filling fraction F=50% versus η=50%

As a summary the information of the gaps of the above considered phononic crystals have been accumulated and plotted as functions of η in Figure 6. As can be seen in this figure the maximum width, equal to 400m/s, of the first band gap occurs at η=0 and the gap dissolved above η=20%. In the middle range the second band gap is dominated above η =5% up to η≈18% with a maximum of 262m/s at η=10%. The third and the long lasting gap start at η=10% and exist until η=50% with a maximum equal to 564 m/s at η=50%. The width of later gap grows continuously by η so that it is the dominated gap above η≈18%. There is also a minor gap which appear above η=10% whose maximum does not excess 98m/s. Finally it should be noted that, however the first and second band gaps have nearly equal maximums, the largest band gap which could be obtain by modifying the volume ratio of rodes A with respect to rode B is belong to third gap at η=50%.

This property is featured in more details in Figure 7 in which the upper and lower boundary corresponding to each gap is depicted as function of η. As shown in this figure, the first and second band gaps lies in the frequency range 1500 m/s-1100 m/s and 2268 m/s-2530 m/s respectively, while in between the third gap lies in range 1558 m/s-2122 m/s. It is notable that no gap is exists below the lower frequency limit of first gap and above the higher frequency limit second band gap (it is tested but not presented here by considering 50 bands in our calculations).

We calculated the density of states in the entire Brillouin zone, which is shown as an example of the results obtained for filling fraction=50% and eta = 50% in Figure 8. According to the obtained results, we observed that this gap is spread throughout the Brillouin zone. The presence and magnitude of this gap in the elastic band structure and density of state clearly show that this band gap extends throughout the Brillouin zone.

In this Figure 7, it is easy to see the bandwidth, lower and upper limits, and the opening and closing points of each band gap in different η values. In the first and third band gaps, the lower limit of the band gap is almost constant and their changes are mainly caused by changes in their upper limit. According to Figure 4, it can be seen that the first, second and third bands are stable and unchanged, and with the movement of the fourth, fifth and sixth modes, the first band gap is closed. After closing the first band gap, these modes remain almost constant and unchanged and play a role as the lower limit of the third band gap. With the stability of these modes, the main changes in the bandwidth of the third band gap are caused by the upward movement of the higher bands. In other words, when the bandwidth of the third band gap increases, the first to sixth modes are constant and unchanged, and the main change of this band gap is caused by the upward movement of the seventh, eighth, ninth and tenth bands. In general, it can be concluded that the addition of the rode A causes the creation of new boundary conditions and the excitation of lateral modes, which this new boundary condition leads to changes in the band gaps.

As can be seen in Figure 4, by changing the η while maintaining the filling fraction of the piezoceramic rods, the dispersion diagram of the piezocomposite changes and shows that the band gaps are very sensitive to these

changes and this parameter can be adjusted to obtain a larger relative bandwidth in the desired frequency range.

From the comparison of Figure 3 (η=0) with the other figures, we can see that with help of this method, we can to create band gaps in different frequency ranges and different widths. In addition, it can be seen that in the η=50 (Figure 4 (f)), the bandwidth of the band gap is 1.43 of the bandwidths in the mode without rode B (η =0) (Figure 3). In addition, it can be seen that in some values of η we have two or three bands at the same time at the different frequency ranges. According to the diagrams, it can be seen that the changes in the bands are due to the displacement of higher modes and their movement towards higher or lower frequencies. In fact, it can be said that the non-uniform volume distribution of piezoceramic rods caused these changes.

With the increase of η, phase b elements appear from zero and their effect gradually increases. Due to the fact that these elements are located in the space between the elements of phase a, the distance between the elements is reduced, and as a result, it is expected that the forbidden gap at low frequency will gradually disappear and be transferred to higher frequencies. As seen in Figure 4, this effect occurs by transferring frequency modes to the forbidden gap. As a result, while the energy of the lowest three frequency bands remains almost constant, the frequency of its upper edge gradually decreases.

The first energy gap is caused by the destructive combination of waves moving in the x or y direction and relatively reflected from the plates containing the phase a elements. Decreasing the volume of phase a elements and increasing the effect of phase b elements on these reflections with increasing η causes the size of this gap to decrease until finally it disappears for η=15 by decreasing the energy of the fourth frequency band.

On the other hand, the second frequency gap appears immediately with the increase of η from zero. Due to the high frequency of this gaffe, its creation can be attributed to the destructive combination of waves that move perpendicular to the planes of phases a and b (along the x or y axes) and are partially reflected from these phases. With the increase of η, the width of this gap increases initially with the increase of η, but finally, this gap closes by reducing the frequency of its upper edge and increasing the energy of its lower edge at η=0.25.

The third energy gap, which is the main one in this research, starts to appear from η=10. This gaffe is caused by the destructive superposition of waves that move along the bisector of the x and y axes and are relatively reflected from the phase elements a and b. The increase in the volume of phase b and the simultaneous decrease in the volume of phase a with the increase of η causes the volume of these two elements to approach each other. As a result, the width of the gap increases continuously with the increase of η, and at η=50, where the volume of the two elements is equal, the gap finds its maximum value. In fact, for η=50, the final grid is a simple square grid, which is rotated by 45 degrees relative to the initial grid of η=0, and the distance between its elements is a/sqrt(2). For this reason, the width of the gap in this case is sqrt(2) equal to the case of η=0

We calculated how in the entire inverted space and observed that this gap has extended in the entire inverted space.

In the past research, such as the research reported by Zhang Hua et al [15], changes in the filling fraction of piezoceramic were usually used to change the bandgap, which causes changes in the functional characteristics of the piezoceramic, such as effective electromechanical coupling coefficient, characteristic impedance, longitudinal velocity and density, but in this case, without changing the piezoceramic filling fraction, the bandwidth and location of the band gaps can be controlled and according to the practical needs, the appropriate bandwidth and the location can be obtained.

3. Conclusion

In this article the phononic band structures of a two-dimensional body center 1-3 piezocomposite consisting of PZT-5H rod and polyethylene terephthalate polymer matrix have been investigated theoretically. By considering the volume fraction of PZT rods as constant as 50% the band structure of the system has been surveyed as function of the ratio η, i.e. the volume fraction of the PZT rod in the center of a unit cell to the total volume of the PZT rods in the unit cell. The results show that for the whole range of variation of η there exist at least one complete band gap in the band structure of the considered structure while no gap exists below f.a=110 m/s and above f.a=2530 m/s. It is shown that the band structure consists of three main band gap (in addition with two minor ones) whose maximums occur at η=0% (first band gap), η=20% (second band gap) and η=50% (third band gap) that the latter one is the largest band gap (equal to 564m/s) of the considered system.

ACKNOWLEDGEMENTS

The authors wish to acknowledge Payame Noor University and Malek Ashtar University for the all support throughout this work.

REFERENCES

1. H. Wang, Y. Li, H. Hui, and T. Rong, “Analysis of electromechanical characteristics of the 1-3-2 piezoelectric composite and 1-3-2 modified structural material,” Ceramics International, vol. 48, no. 15, pp. 22364–22375, Aug. 2022, https://doi.org/10.1016/j.ceramint.2022.04.238
2. B. Amanat, “Improvement of the Effective Parameters of 1-3 Piezocomposite Using Multi-Layer Polymer and PMN-PT Relaxor Single Crystal,” Advanced Ceramics Progress, vol. 8, no.

2, pp. 61–72, Jun. 2022, .https://doi.org/10.30501/acp.2022.355196.1099

3. J. Lv et al., “Cold ablated high frequency PMN-PT/Epoxy 1-3 composite transducer,” Applied Acoustics, vol. 188, p. 108540, Jan. 2022, https://doi.org/10.1016/j.apacoust.2021.108540
4. P. Tize Mha, P. Maréchal, G. E. Ntamack, and S. Charif d’Ouazzane, “Homogenized electromechanical coefficients and effective parameters of 1–3 piezocomposites for ultrasound imaging transducers,” Physics Letters A, vol. 408, p. 127492, Aug. 2021, https://doi.org/10.1016/j.physleta.2021.127492
5. A. Behera, “Piezoelectric Materials,” in Advanced Materials: An Introduction to Modern Materials Science, A. Behera, Ed., Cham: Springer International Publishing, 2022, pp. 43–76. http://dx.doi.org/10.1007/978-3-030-80359-9_2
6. C. Zhou, J. Zhang, D. Liu, and Z. Zhang, “Novel 1–3 (K,Na)NbO3-based ceramic/epoxy composites with large thickness-mode electromechanical coupling coefficient and good temperature stability,” Ceramics International, vol. 47, no. 4, pp. 4643–4647, Feb. 2021, https://doi.org/10.1016/j.ceramint.2020.10.031
7. Y.-Z. Wang, F.-M. Li, K. Kishimoto, Y.-S. Wang, and W.-H. Huang, “Wave band gaps in three-dimensional periodic piezoelectric structures,” Mechanics Research Communications, vol. 36, no. 4, pp. 461–468, Jun. 2009, https://doi.org/10.1016/j.mechrescom.2009.01.003
8. S. L. Vatanabe and E. C. N. Silva, “Design of phononic band gaps in functionally graded piezocomposite materials by using topology optimization,” in Behavior and Mechanics of Multifunctional Materials and Composites 2011, SPIE, Apr. 2011, pp. 268–277. https://doi.org/10.1117/12.878851
9. O. Sigmund and J. Jensen, “Systematic design of phononic band-gap materials and structures by topology optimization,” Philosophical transactions. Series A, Mathematical, physical, and engineering sciences, vol. 361, pp. 1001–19, Jun. 2003, https://doi.org/10.1098/rsta.2003.1177
10. M.-L. Wu, L.-Y. Wu, W.-P. Yang, and L.-W. Chen, “Elastic wave band gaps of one-dimensional phononic crystals with functionally graded materials,” Smart Materials and Structures, vol. 18, p. 115013, Sep. 2009, https://doi.org/10.1088/0964-1726/18/11/115013.
11. E. J. P. Miranda and J. M. C. Dos Santos, “Wave attenuation in 1-3 phononic structures with lead-free piezoelectric ceramic inclusions,” Physica B: Condensed Matter, vol. 631, p. 413642, Apr. 2022, https://doi.org/10.1016/j.physb.2021.413642.
12. Z. Hou, F. Wu, and Y. Liu, “Phononic crystals containing piezoelectric material,” Solid State Communications, vol. 130, no. 11, pp. 745–749, Jun. 2004, https://doi.org/10.1016/j.ssc.2004.03.052.
13. Z. Qian, F. Jin, Z. Wang, and K. Kishimoto, “Dispersion relations for SH-wave propagation in periodic piezoelectric composite layered structures,” International Journal of Engineering Science, vol. 42, no. 7, pp. 673–689, Apr. 2004, https://doi.org/10.1016/j.ijengsci.2003.09.010.
14. S. L. Vatanabe, G. H. Paulino, and E. C. N. Silva, “Maximizing phononic band gaps in piezocomposite materials by means of topology optimization,” The Journal of the Acoustical Society of America, vol. 136, no. 2, p. 494, Aug. 2014, https://doi.org/10.1121/1.4887456.
15. Z.-H. Qian, F. Jin, F.-M. Li, and K. Kishimoto, “Complete band gaps in two-dimensional piezoelectric phononic crystals with {1–3} connectivity family,” International Journal of Solids and Structures, vol. 45, no. 17, pp. 4748–4755, Aug. 2008, https://doi.org/10.1016/j.ijsolstr.2008.04.012.
16. J. M. T. Thompson and O. Sigmund, “Topology optimization: a tool for the tailoring of structures and materials,” Philosophical Transactions of the Royal Society of London. Series A: Mathematical, Physical and Engineering Sciences, vol. 358, no. 1765, pp. 211–227, Jan. 2000, http://dx.doi.org/10.1098/rsta.2000.0528.
17. S. Halkjaer, O. Sigmund, and J. Jensen, “Inverse design of phononic crystals by topology optimization,” Zeitschrift Fur Kristallographie - Z KRISTALLOGR, vol. 220, pp. 895–905, Oct. 2005, http://dx.doi.org/10.1524/zkri.2005.220.9-10.895.
18. S. Halkjær, O. Sigmund, and J. Jensen, “Maximizing band gaps in plate structures,” Structural and Multidisciplinary Optimization, vol. 32, pp. 263–275, Oct. 2006, http://dx.doi.org/10.1007/s00158-006-0037-7.
19. C. Rupp, A. Evgrafov, K. Maute, and M. Dunn, “Design of phononic materials/structures for surface wave devices using topology optimization,” Structural and Multidisciplinary Optimization, vol. 34, pp. 111–121, Aug. 2007, http://dx.doi.org/10.1007/s00158-006-0076-0.
20. A. K. Vashishth and V. Gupta, “Wave propagation in transversely isotropic porous piezoelectric materials,” International Journal of Solids and Structures, vol. 46, no. 20, pp. 3620–3632, Oct. 2009, https://doi.org/10.1016/j.ijsolstr.2009.06.011.
21. Y.-Z. Wang, F.-M. Li, W.-H. Huang, and Y.-S. Wang, “Effects of inclusion shapes on the band gaps in two-dimensional piezoelectric phononic crystals,” Journal of Physics: Condensed Matter, vol. 19, p. 496204, Nov. 2007, https://doi.org/10.1088/0953-8984/19/49/496204.
22. Y.-S. Wang, “Calculation of band structures for surface waves in two-dimensional phononic crystals with a wavelet-based method,” Phys. Rev. B, vol. 78, Sep. 2008, https://doi.org/10.1103/PhysRevB.78.094306.
23. T. Vu Quoc et al., “DFT study on some polythiophenes containing benzo[d]thiazole and benzo[d]oxazole: structure and band gap,” Designed Monomers and Polymers, vol. 24, no. 1, pp. 274–284, Jan. 2021, https://doi.org/10.1080/15685551.2021.1971376.
24. C. Comi and J.-J. Marigo, “Homogenization Approach and Bloch-Floquet Theory for Band-Gap Prediction in 2D Locally Resonant Metamaterials,” Journal of Elasticity, vol. 139, Apr. 2020, https://doi.org/10.1007/s10659-019-09743-x.
25. J. O. Vasseur, B. Djafari-Rouhani, L. Dobrzynski, M. S. Kushwaha, and P. Halevi, “Complete acoustic band gaps in periodic fibre reinforced composite materials: the carbon/epoxy composite and some metallic systems,” Journal of Physics Condensed Matter, vol. 6, pp. 8759–8770, Oct. 1994, https://doi.org/10.1088/0953-8984/6/42/008.